Extremophiles (2006) 10:139–148
DOI 10.1007/s00792-005-0484-x

ORIGINAL PAPER

Jana Tatur · Peter-Leon Hagedoorn
Marieke L. Overeijnder · Wilfred R. Hagen

A highly thermostable ferritin from the hyperthermophilic archaeal anaerobe *Pyrococcus furiosus*

Received: 7 July 2005 / Accepted: 18 September 2005 / Published online: 10 December 2005

Abstract A ferritin from the obligate anaerobe and hyperthermophilic archaeon *Pyrococcus furiosus* (optimal growth at 100°C) has been cloned and overproduced in *Escherichia coli* to one-fourth of total cell-free extract protein, and has been purified in one step to homogeneity. The ferritin (PfFtn) is structurally similar to known bacterial and eukaryal ferritins; it is a 24-mer of 20 kDa subunits, which add up to a total Mr 480 kDa. The protein belongs to the non-heme type of ferritins. The 24-mer contains approximately 17 Fe (as isolated), 2,700 Fe (fully loaded), or <1 Fe (apoprotein). Fe-loaded protein exhibits an EPR spectrum characteristic for superparamagnetic core formation. At 25°C $V_{max} = 25$ μmole core Fe^{3+} formed per min per mg protein when measured at 315 nm, and the $K_{0.5} = 5$ mM Fe(II). At 0.3 mM Fe(II) activity increases 100-fold from 25 to 85°C. The wild-type ferritin is detected in *P. furiosus* grown on starch. PfFtn is extremely thermostable; its activity has a half-life of 48 h at 100°C and 85 min at 120°C. No apparent melting temperature was found up to 120°C. The extreme thermostability of PfFtn has potential value for biotechnological applications.

Keywords Ferritin · Hyperthermophile · *P. furiosus* · Thermostability · Anaerobe

Communicated by F. Robb

J. Tatur · P.-L. Hagedoorn · M. L. Overeijnder · W. R. Hagen (✉)
Department of Biotechnology,
Delft University of Technology,
Julianalaan 67, 2628 BC Delft,
The Netherlands
E-mail: w.r.hagen@tnw.tudelft.nl
Tel.: +31-15-2785051
Fax: +31-15-2782355

Introduction

Ferritins are present in a wide variety of organisms: bacteria, archaea, fungi, plants, insects and vertebrates. Their main role is presumably iron storage; excess of Fe^{2+} from a cell environment is internalized and then taken up by ferritin, oxidized, and stored as ferrihydride in its cavity until the cell needs it. Upon addition of reducing equivalents, iron is released. This function of ferritins is a key part of the homeostasis machinery of higher organisms that ensures the right balance of iron in the organism. Iron is an essential nutrition element as it is used for the biosynthesis of a myriad of prosthetic groups such as heme or iron-sulfur clusters. At the same time iron excess in higher organisms leads to oxidative stress, which may result in permanent cell damage. There are two major classes of ferritin: non-heme ferritin and heme-containing ferritin or bacterioferritin. Non-heme ferritin, which is normally designated as ferritin, is present in many different species from prokaryotes to man. Bacterioferritin has been found only in bacteria and fungi. Ferritin and bacterioferritin are globular shells consisting of 24 subunits with approximate subunit size of 20 kDa, and they can theoretically bind up to 4,500 Fe(III) ions per 24-mer (Crichton 2001). A bacterioferritin harbors up to 12 heme groups per 24-mer (Frolow et al. 1994). An additional or alternative function for both types of ferritins in anaerobic organisms is believed to be a protection from traces of oxygen and its derivatives (Carrondo 2003; Romão et al. 2000). There is a related group of proteins, which form smaller shells of 12-mers and can incorporate ca. 500 Fe atoms in a smaller core structure (Zhao et al. 2002). These proteins are frequently associated with the protection of DNA against oxidative damage, and they are named DNA-binding protein from starved cells, or Dps (Almiron et al. 1992).

Recent research on ferritins has been directed towards the elucidation of the differences in the functions of bacterioferritins and ferritins, the role of

ferritins in anaerobic organisms, and understanding the mechanism of iron incorporation. Crystallographic structures are available on ferritins, bacterioferritins, and Dps's from several species (reviewed in Carrondo 2003). Archaeal–structural data are thus far limited to a ferritin from the sulfate-reducing thermophile *Archaeoglobus fulgidus* (Johnson et al. 2005) and a Dps-like ferritin from the mesophilic halophile *Halobacterium salinarum* (Zeth et al. 2004). The latter study provides the first detailed description of a possible route from initially bound Fe(II), via oxidation of the ferroxidase site inside each subunit, to the formation of a specific iron-oxo cluster at a nucleation site (Zeth et al. 2004).

In the present study the putative ferritin gene from the obligate anaerobe and hyperthermophilic archaeon *Pyrococcus furiosus* has been cloned and overproduced in *Escherichia coli*. The protein purified to homogeneity showed to be a functional non-heme ferritin. The protein is the most thermostable ferritin known so far. A preliminary X-ray characterization of this ferritin has been performed (Matias et al. 2005) and its structure solution is on the way.

Experimental procedures

Protein production

Wild-type *P. furiosus* DSM 3638 cells were cultivated anaerobically at 92°C on starch as carbon source in the presence of 0.5 M NaCl as previously reported (Arendsen et al. 1995). Cell-free extract was prepared as outlined in (Hagedoorn et al. 1999) by osmotic shock of the *P. furiosus* cells. The putative structure gene for ferritin from *P. furiosus* (SWISS-Prot primary accession number Q8U2T8) was cloned into pET24a(+) vector (Novagen) and the protein was overproduced in BL21-CodonPlus (DE3)-RIL *E. coli* host cells (Stratagene) using the T7 promoter-lac operator IPTG induced system as earlier described (Matias et al. 2005). The produced recombinant *E. coli* cells were broken with a cell disruptor (Constant Systems) and ferritin was purified in one step by heat treatment at 100°C for 30 min. The precipitated proteins were removed by centrifugation. The supernatant was buffer-exchanged into 50 mM Hepes, pH 7, NaCl 250 mM (working buffer) and concentrated over Amicon, YM-100, to give the final preparation of the protein.

Gel electrophoresis

The SDS, native, and isoelectric focusing electrophoresis was performed on a Phast System (Amersham Biosciences) using 10–15% pre-cast gradient gels and 3–9 pI for IEF. The markers mix (Amersham Biosciences) consisted of thyroglobuline (porcine thyroid, 0.76 mg/ml), ferritin (horse spleen, 0.5 mg/ml), catalase (bovine liver, 0.36 mg/ml), lactate dehydrogenase (bovine heart, 0.48 mg/ml) and albumin (bovine serum, 0.40 mg/ml) for native gels and phosphorylase b (rabbit muscle, 0.67 mg/ml), albumin (bovine serum, 0.83 mg/ml), ovalbumin (chicken egg white, 1.47 mg/ml), carbonic anhydrase (bovine erythrocyte, 0.83 mg/ml), trypsin inhibitor (soybean, 0.80 mg/ml), and α-lactalbumin (bovine milk, 1.16 mg/ml) for SDS gels. For SDS electrophoresis the sample was boiled for 5 min prior to applying to the gel to stimulate dissociation of the subunits. Protein was stained with Coomassie Brilliant Blue. Iron staining of native gels was done with Prussian blue: freshly made 2.5% potassium ferrocyanide with 2.5% of hydrochloric acid. Staining of the wild-type ferritin was performed by running two lanes of the sample on the native gel, cutting the gel in two halves and staining one half with CBB and the other one with Prussian blue.

Molecular mass determination

Molecular mass (Mr) of the protein was determined with Superdex 200 HR 10/30 gel filtration chromatography calibrated with blue dextran (6 mg/ml), thyroglobuline (6 mg/ml), horse spleen ferritin (12 mg/ml), catalase (7 mg/ml), aldolase (10 mg/ml), and bovine heart cytochrome *c* (2 mg/ml) as markers. The experiment was performed with 20 mM Tris/HCl buffer pH 8, containing 0.15 M NaCl at a flow rate of 0.5 ml/min. The Mr was also determined from SDS and native gel electrophoresis.

N-terminal sequencing

The N-terminal amino acid sequencing was performed via Edman degradation on a sample blotted onto PVDF membrane.

Activity assay

The ferroxidase activity of the recombinant ferritin was measured at 25–85°C by following the increase in absorption at 315 nm after the addition of iron (II) sulfate. The reaction was performed in the working buffer. The iron sulfate solution was freshly prepared in water, containing 0.1% HCl (v/v) for stabilizing the Fe(II) against auto-oxidation (Baaghil et al. 2003), and made anaerobic by flushing with argon. The specific activity was assayed in units per mg of protein where one unit is the number of μmoles of Fe^{2+} converted into core Fe^{3+} per minute. The extinction coefficient used was $\varepsilon_{315} = 2{,}200\ M^{-1}\ cm^{-1}$ (Bonomi et al. 1996).

Spectroscopy

UV-visible spectra were recorded with a Hewlett Packard 8453 photodiode array spectrophotometer; steady-state kinetics was followed on a fiber optics Avantes

DM-2000 spectrophotometer. EPR spectra were recorded on a Bruker 200 D EPR spectrometer equipped with a home-built cryogenic flow system and with data collection and peripheral equipment as described in (Pierik et al. 1991). Spin quantitation was done versus a copper standard i.e., 10.0 mM $CuSO_4$, 10 mM HCl, 2 M $NaClO_4$. Effective *g* values of high-spin Fe(III) were estimated with the program RHOMBO (Hagen 1992).

Thermostability

The thermostability of the ferritin iron incorporation activity was studied by incubating the protein at 100°C in a water bath or autoclaving at 120°C and withdrawal of samples after specific time intervals followed by activity assay at 30°C. Protein was kept in HPLC bottles closed with rubber covers and capped. Samples were withdrawn with a syringe to prevent evaporation and concentration of the protein. In the autoclaving experiment the time scale is the actual autoclaving time at 120°C and does not include heating and cooling time of the autoclave. The data points were fitted (Igor 5.0) to a sigmoidal process. Differential scanning calorimetry was performed with a MicroCal VP-DSC.

Analytical determinations

Protein concentration was determined with bicinchoninic acid using bovine serum albumin as the standard (BCA Kit, Pierce). The possible interference of iron in the iron-loaded samples was controlled by precipitation with trichloroacetic acid (BCA Kit instructions, Pierce). Iron was determined based on Hennessy et al. (1984) and Pierik et al. (1992) as follows: to 30 µl of protein of approximately 4 µM concentration (24-mer) 3 µl of HCl was added in order to disrupt the protein. After incubation at room temperature for a few minutes, the sample was centrifuged (13,400 rpm, 15 min). The supernatant was collected and 50 µl of 3 M sodium acetate and 5 µl of 1 M ascorbic acid, pH 5–6 were added. After taking a blank spectrum, 5 µl of 3 mM ferene was added to the mixture. Iron concentration was calculated using the extinction coefficient of the iron-ferene complex of 35,500 M^{-1} cm^{-1} at 593 nm.

Preparation of apo-ferritin

The apo-ferritin was prepared based on (Bauminger et al. 1991; Dawson et al. 1986) by reducing the protein solution (up to 0.5 µmole ferritin 24-mer) with an anaerobic 50 mM sodium dithionite solution (200 ml) in the working buffer through a YM-100 membrane in a 50 ml Amicon cell. The resulting concentrate was collected anaerobically into a glass bottle sealed with a butyl-rubber stopper and an equal amount of a fresh sodium dithionite solution was added. After overnight incubation an anaerobic 0.5% 2,2′-bipyridyl solution in ethanol was added to the sample in order to complex the remaining Fe(II). The resulting 10 ml mix was extensively dialyzed against the working buffer in 12 ml dialysis Slide-A-Lyser cassettes (Pierce) and concentrated in an Amicon cell over YM-100.

Iron incorporation

In order to determine the maximum iron storage capacity of PfFtn, aliquots of low iron concentrations were added stepwise to low protein concentration in order to avoid precipitation of ferritin (Treffry et al. 1978). Conditions for iron incorporation were as described under "Activity assay". To 0.1–0.15 mg/ml apo-ferritin 0.3 mM iron sulfate was added. The iron uptake was conducted at 25°C and monitored spectrophotometrically at 315 nm. Another aliquot of Fe^{2+} was added to the mixture when the iron uptake graph reached a plateau value. Additions were repeated until the solution started to become turbid as an indication of ferritin-full iron saturation followed by rust formation from surplus iron and protein precipitation. The iron storage capacity was screened on multiple samples in which iron concentration was increased in steps of 50 Fe/24-mer. Iron determination was then performed on the sample with highest iron loading that showed no precipitation after 3 days of incubation in air.

Bioinformatics tools

Amino acid and DNA sequences were explored with the BLAST program (Altschul et al. 1997) at the Institute for Genomic Research database (TIGR, http://www.tigr.org). The multiple alignment was performed with Clustal W (Thompson et al. 1994) software at the Network Protein Sequence analysis website (Combet et al. 2000). Swiss-Prot database (http://au.expasy.org/sprot) was used to obtain the accession numbers of the proteins.

Results

Detection of wild-type ferritin

The present study on recombinant ferritin from *P. furiosus* was motivated by the discovery of the wild-type ferritin expression. This was observed in native gel electrophoresis of cell-free extract from *P. furiosus* after staining for iron. The only protein band developed on the gel upon iron staining was a band of ca. 440 kDa, next to the horse spleen ferritin band from the marker mix (Fig. 1a). Attempts to purify native ferritin did not result in sufficient amount of protein for biochemical/biophysical characterization and therefore the recombinant approach has been chosen.

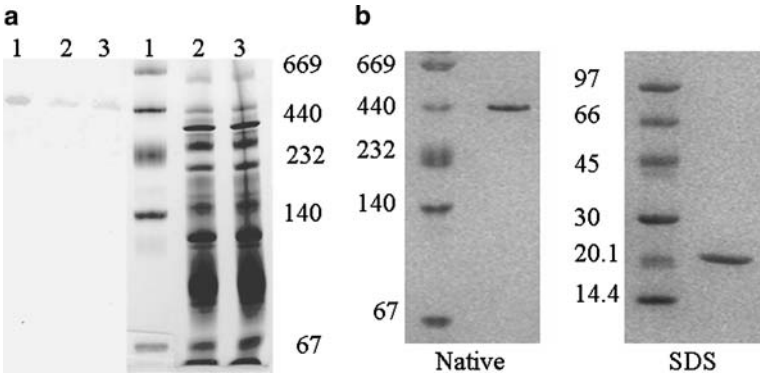

Fig. 1 Wild-type and recombinant ferritin from *P. furiosus*. **a** Wild-type ferritin. Native gel was stained with coomassie brilliant blue for protein (*right three lanes*) and Prussian blue for iron (*left three lanes*). *1*Marker mix, *2* and *3* two different preparations of cell-free extract (CFE). **b** Recombinant ferritin. Native and SDS gel electrophoresis. Molecular masses of markers are in kDa. Protein amounts used were: *lane 1* 4 µl marker mix (see Experimental procedures for concentrations); *lane 2* 144 µg CFE; *lane 3* 160 µg CFE; **b** native, 4 µl marker mix and 24 µg purified PfFtn; **b** SDS, 2 µl marker mix and 18 µg purified PfFtn

Table 1 Purification table

	V (ml)	Concent. (mg/ml)	Total protein (mg)	Specific act (U/mg)	Purification fold	Yield (%)	Ferritin (%) of total protein
CFE	153.0	36.0	5508.0	0.51	1.0	100.0	27.5
Heat step	31.0	16.0	496.0	1.84	3.6	32.7	100.0

Activities were measured at 25°C

Expression and purification of recombinant ferritin

The putative ferritin gene from *P. furiosus* was cloned and expressed as a functional protein in *E. coli* cells. The overexpressed ferritin accounted for one-fourth of the total protein in the cell-free extract. This was estimated based on 100% purity of the purified ferritin as judged by gel electrophoresis (Fig. 1b) and a ca. fourfold purification factor (Table 1). A heating step is sometimes used for ferritin purifications (Andrews et al. 1993; Hudson et al. 1993; Levi et al. 1987; Rocha et al. 1992) due to the protein's relatively high thermal stability. In our case the choice to use the heating step was especially motivated by hyperthermostability of *P. furiosus*, growing optimally at 100°C (Fiala et al. 1986). Initially the protein was purified using a heating step at 80°C, followed by Superdex 200 gel filtration chromatography, but it was subsequently found that the extreme thermostability of PfFtn (see below) allowed isolation in one step via incubation of the protein in a 100°C water bath for 30 min. The heating step produced pure protein, based on gel electrophoresis.

The identity of the purified recombinant protein with ferritin from *P. furiosus* was checked by SDS gel electrophoresis of extract from *E. coli* cells grown with and without induction, by the ferritin assay of iron incorporation, and by N-terminal amino acid sequence determination of the purified recombinant protein. The SDS gel showed a bright band appearing in extract from induced cells only (not shown). Activity assays were performed on cell-free extracts from two types of *E. coli* cells, with and without the recombinant ferritin construct, cultivated under the same conditions. Both the cell-free extracts were subjected to a heating step of 80°C and centrifugation for removal of precipitated proteins. The activity measurement (25°C) resulted in more than 130 times higher specific activity in the recombinant cells (1.502 U/mg) than in construct-deficient host cells (0.011 U/mg). The N-terminal sequence of the purified recombinant ferritin was identical to that in the genome database: MLSERMLKALNDQLNRELYS. The N-terminal Met is not removed by *E. coli*.

Quaternary structure

The molecular mass determined from the SDS gel was 20 kDa and from the native gel it was 440 kDa (Fig. 1b). The predicted molecular mass of the translated structural gene was 20,309 Da; the molecular mass determined with mass spectrometry was 20,397 Da. Analytical gel filtration chromatography gave an estimated molecular mass of 412 kDa for apoferritin and 438 kDa for ferritin fully loaded with iron. Within experimental uncertainty this is consistent with the protein being a 24-mer of ca. 20 kDa subunits as for other known ferritins. For further calculations we assume a protein molecular mass of 480 kDa with a subunit size of 20 kDa.

Iron staining

A native gel with apoferritin, ferritin as isolated, and ferritin loaded with 1,152 Fe^{2+}/24-mer was run in parallel and stained for protein and iron (not shown). Protein staining revealed all three samples with the same electrophoretic mobility. Iron staining showed loaded ferritin, a very light band of ferritin as isolated, and a band of the horse spleen ferritin present in the marker mix. Apoferritin could not be detected on the iron-staining gel.

Isoelectric focusing

Isoelectric focusing of apo-ferritin and Fe-loaded ferritin afforded the same value of pI = 4.5, indicating that there is probably no iron binding on the outer side of the protein.

Iron incorporation

The recombinant ferritin as isolated from *E. coli* contains ca. 17 Fe per 24-mer. After reductive de-metallation with α,α′-bipyridyl (Bauminger et al. 1991) the apoferritin contains < 1 Fe per 24-mer. Prolonged loading of the as isolated protein with Fe^{2+} affords a maximal loading of ca. 2,700 Fe per 24-mer. The latter value was obtained for a sample incubated for 3 days at 22°C since the last iron addition. Ferritin samples loaded with higher amounts of iron, although they looked clear on the first day, on the second day would show precipitation. Apoferritin was also loaded with iron but showed lower iron incorporation capacity than as isolated ferritin; it could incorporate approximately 600 iron ions less than as isolated ferritin.

Spectroscopy

The UV-visible spectrum of the apoprotein has absorption maxima at 227, 280 nm, and a shoulder at 290 nm (Fig. 2). After addition of $FeSO_4$ the absorption increases (dashed line) by the growing-in of a very broad absorption peak approximately centered at 250 nm and extending all the way up to ca. 550 nm. This spectrum from the ferrihydride core is readily quantified at a wavelength of 315 nm (Bonomi et al. 1996) where the protein absorption is zero. In Fig. 2 the dashed spectrum corresponds to an intermediate state in iron incorporation. The shape of the iron-core spectrum appears to be invariant over the course of the incorporation (not shown).

Figure 3 shows the dependence of the iron incorporation rate, followed at 315 nm, on the substrate concentration. The measurements were performed at 25°C. This experiment could not be done at higher temperatures (up to 85°C) due to fast non-enzymatic Fe^{2+} oxidation when Fe^{2+} is used in concentrations of the order of 10 mM. The initial part of the graph is distinctly non-Michaelis-Menten, suggestive of cooperativity. A fit to the Hill equation $[SA = SA_{max}\cdot[S]^n/([S]^n + K_{0.5}^n)$, where SA is the specific activity (initial rate), S is the concentration of the substrate, $K_{0.5}$ is the substrate concentration which gives half maximal activity, and n is the Hill coefficient] gives $V_{max} = 25$ U/mg, $K_{0.5} = 5$ mM, and $n = 2$, where $n > 1$ is a measure for positive cooperativity. The specific activity at low Fe(II) concentration (300 μM) at 85°C (176 U/mg) is approximately 100 times higher than at 25°C (1.8 U/mg).

The EPR spectrum of the ferritin, as isolated, is presented in Fig. 4, trace a. In addition to a small peak at $g = 4.3$ (ca. 1,570 Gauss) of insignificant integrated intensity, there are two asymmetric peaks at low field with approximate effective g values of ≈7.3 and 5.8. Such features are characteristic for high-spin mononuclear Fe(III) at a site of intermediate rhombicity [i.e., with a rhombicity parameter $0 < E/D < 1/3$; see (Hagen 1992)]. Theory predicts sets of effective g values for the transitions within the three Kramers doublets of high-spin Fe(III) (Hagen 1992), and for rhombicity $E/D = 0.065$ low-field peaks at $g = 7.4$ and 5.9 are predicted with comparable peak area from the transitions within

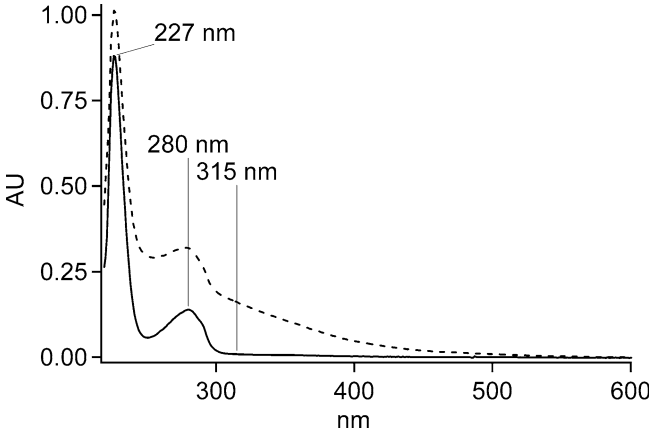

Fig. 2 UV-visible spectra of recombinant *P. furiosus* ferritin. Apoferritin (*solid*) and Fe-loaded ferritin (*dashed*). The protein concentration was 0.07 μM and added Fe^{2+} was 186 μM

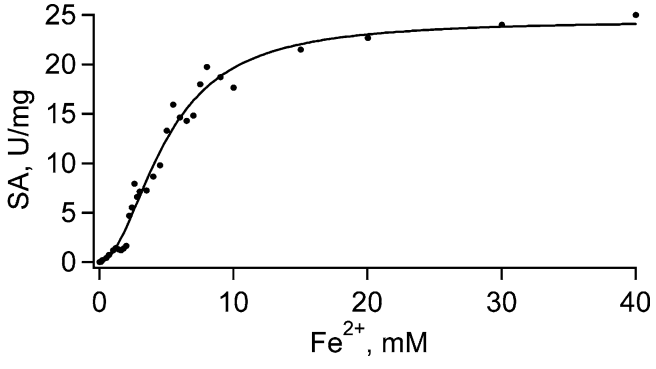

Fig. 3 Steady-state kinetics of *P. furiosus* ferritin. Kinetics was followed at 315 nm, $T = 25$°C. Specific activity (initial rates) is given as a function of substrate concentration. Protein concentration was 10.4 μM

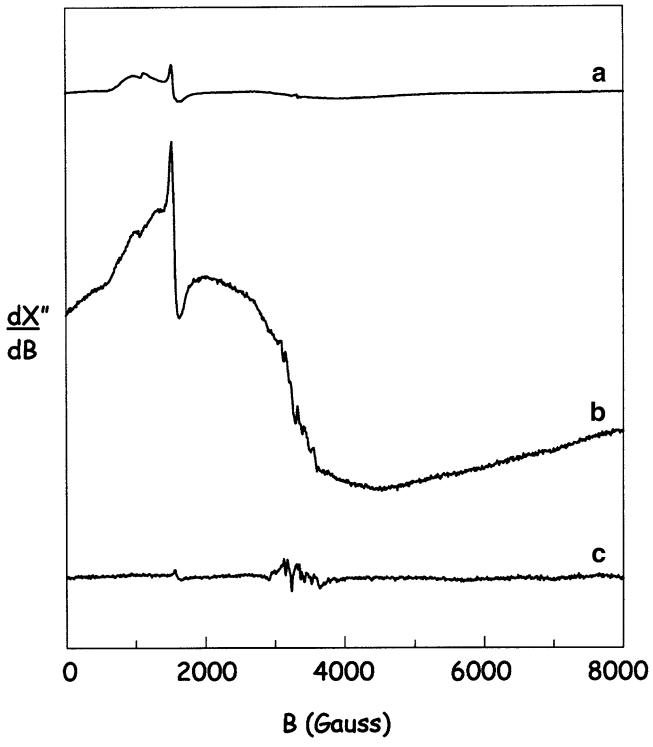

Fig. 4 EPR spectra of *P. furiosus* ferritin expressed in *E. coli*: **a** as isolated with ca. 17 Fe/24-mer; **b** after aerobic loading with 1,140 $FeSO_4$; **c** apo-ferritin with < 1 Fe/24-mer obtained after removal of iron from the as isolated protein with bipyridyl under reducing conditions followed by dialysis and re-aeration. The amplitudes of the spectra are normalized with respect to protein concentration (30, 12, 15 mg/ml, respectively). EPR conditions were: microwave frequency, 9.43 GHz; microwave power, 200 mW; modulation frequency, 100 kHz; modulation amplitude, 6.3 Gauss; temperature, ca. 110 K

the two lowest doublets, while the transition within the highest doublet has insignificant intensity. Remarkably, the signal is quite similar to one previously reported for native wild-type bacterioferritin from *E. coli*, where it was putatively assigned to mononuclear Fe(III) located at or near the ferroxidase center (Cheesman et al. 1993; Le Brun et al. 1993). The ferroxidase center is a specific binding site for two Fe inside each subunit and is thought to be the site of oxidation of iron by, e.g., molecular oxygen.

When the ferritin is oxidatively loaded with iron (1,150 Fe) the spectrum of trace b is obtained. In addition to the mononuclear Fe(III) signal an extremely broad feature is found which is typical for superparamagnetism in the mineral core of ferritin and bacterioferritin proteins (Boas et al. 1971; Cheesman et al. 1992; Deighton et al. 1991; Voskoboynik 1997; Wajnberg et al. 2001; Weir et al. 1985). The broad feature is also detectable, with much lower intensity, in the spectrum of as isolated ferritin (trace a), which means that the protein obtained from *E. coli* does not only carry mononuclear Fe(III) but also has a small ferrihydride core. Superparamagnetic systems are characterized by a blocking temperature below which individual crystalline domains become magnetically ordered either ferromagnetically of antiferromagnetically. The blocking temperature for ferritins has been estimated to be ca. 25 K (Wajnberg et al. 2001). Indeed, when the loaded *P. furiosus* ferritin or the as isolated ferritin are measured at a temperature of 4.2 K, the spectrum of the core has disappeared (not shown) indicating full antiferromagnetic coupling at this temperature.

Treatment of the as isolated ferritin with bipyridyl under reducing conditions followed by dialysis and subsequent exposure to air affords the spectrum of trace c, which is indicative of the complete removal of all iron, and this is consistent with the chemical iron determination of < 1 Fe per 24-mer. The small multiline spectrum around $g = 2$ (ca. 3,370 Gauss) is from a trace amount of contaminating Mn(II); it is also found in the Fe-loaded sample.

Thermostability

The activity of the recombinant ferritin proved to be highly thermostable. The protein showed no significant drop in its core formation activity during the first 11 h of incubation at 100°C or the first 36 min autoclaving at 120°C. The half-life times were 48 h and 85 min, respectively [Fig. 5, data points were fitted to a sigmoidal curve $SA = SA_{max}/[1 + \exp((t_{½} - t)/k)]$, where $t_{½}$ is the time after which the protein retains 50% of its activity and k is a denaturation rate]. Ferritin did not show a melting temperature when analyzed with differential scanning calorimetry from 20 to 120°C. The protein was also tested for stability against freezing-thawing and showed no drop in activity after 3 cycles.

Sequence alignment

In Fig. 6 the amino acid sequence of ferritin from *P. furiosus* is aligned with that of *A. fulgidus* ferritin (47% identity, 71% similarity), *E. coli* cytoplasmic ferritin (36 and 56%), human ferritin heavy chain (29 and 47%) and *E. coli* bacterioferritin (17 and 33%). The numbering in Fig. 5 is according to the *P. furiosus* sequence. The typical patterns of ligands to Fe_A^{3+}–Fe_B^{3+} in the ferroxidase center (Romão 2003) are highlighted in gray. These are E_{17}, Y_{24}, E_{50}, and H_{53} in the characteristic motif EXXH, E_{94}, and finally Q_{127} and E_{130} arranged in the motif QXXE. The latter motif is modified in bacterioferritin, which has Glu_{127} and His_{130} making it EXXH. The Glu_{49} in *P. furiosus* and *E. coli* and Glu_{51} in *A. fulgidus* ferritins and Glu_{61} in human ferritin are conserved. In the crystal structure of *E. coli* ferritin Glu_{49} is a ligand to a third iron, Fe_C^{3+}, obtained by soaking the crystals in Fe^{2+} solution. This position was not occupied when crystals were soaked with Zn^{2+} (Romão 2003; Stillman et al. 2001). In the case of human ferritin the highlighted residues are putative ligands to

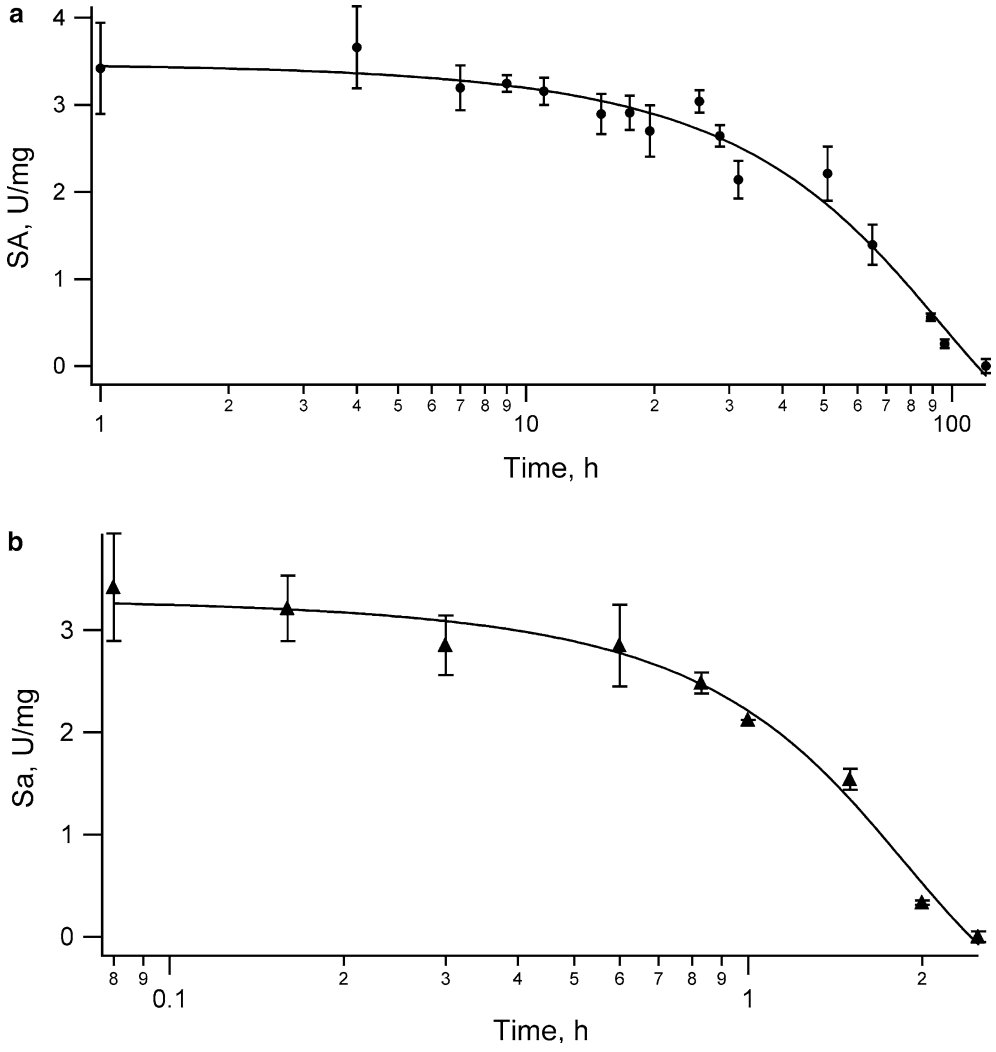

Fig. 5 Thermostability of *P. furiosus* ferritin. The stability was analyzed by incubating the protein at 100°C in a water bath (**a**) or at 120°C in an autoclave (**b**) and withdrawal of samples after specific time intervals followed by measuring the iron incorporation activity (30°C) of the protein in a time course. Protein concentration was 0.3 μM and iron (II) was 0.3 mM

the ferroxidase center since no metal ions were yet found in the site (Hempstead et al. 1997; Romão 2003).

Discussion

A ferritin in *P. furiosus*

In the present study it is shown that the strict anaerobic hyperthermophilic archaeon *P. furiosus* produces ferritin and that its gene can be cloned and expressed as a functional ferritin to very high levels in aerobically grown *E. coli* cells. The purified 24-meric protein is competent in vitro in binding Fe(II) and converting it to Fe(III) in a superparamagnetic core mineral. The PfFtn iron storage capacity of ca. 2,700 Fe/holomer is the same as that of *E. coli* bacterioferritin (2,700 Fe) (Baaghil et al. 2003) and slightly higher than that of *E. coli* ferritin (2,000 Fe) (Hudson et al. 1993). Although theoretically the size of ferritins' inner cavity allows storage of up to 4,500 Fe, in practice the capacity is less than 3,000 (Treffry et al. 1978).

The paradigmatic function of ferritin in higher eukaryotes is storage/release of iron as part of iron homeostasis machinery. The storage requires molecular oxygen; release is dependent on physiological reductant(s) that is yet to be identified. The superoxide anion radical is a mild reductant in vitro (Boyer et al. 1987). Ferritin or ferritin-like proteins are also ubiquitously found in the prokaryotic world; however, a physiological role is not clearly established especially for anaerobic species. *P. furiosus* is an obligate anaerobe, therefore, a putative iron storage function of its ferritin would require a different oxidant than O_2. As with other anaerobes, a candidate for this oxidative function is not yet obvious. Ferritin-like proteins have repeatedly been implicated in oxidative-stress protection either as general scavengers of O_2 and derived species or as specific guardians against DNA cleavage (Rocha et al. 1992; Romão et al. 2000; Smith 2004). As an inhabitant of shallow offshore marine niches (Fiala et al. 1986), *P. furiosus* may well have to occasionally deal with oxidative stress, as is indicated by the presence of a number of genes encoding proteins with putative

Fig. 6 Amino acid sequence alignment of *P. furiosus* ferritin, *E. coli* cytoplasmic ferritin, *A. fulgidus* ferritin, human ferritin heavy chain, and *E. coli* bacterioferritin. Primary accession numbers are Q8U2T8, P23887, O29424, P02794, and P11056, respectively. The residue numbers are according to the *P. furiosus* sequence. *Highlighted* is the alignment with the crystallographically identified ligands to the ferroxidase center in *E. coli* cytoplasmic ferritin (reviewed in Romão 2003)

functions in protection against oxygen species, e.g., superoxide reductase (Adams et al. 2002; Jenney et al. 1999) and rubredoxin:O_2 oxidoreductase (Ma et al. 1999) or rubrerythrin (Tempel et al. 2004). As a working hypothesis, we may now add ferritin to this list with the caveat that physiological data to support this view are yet to be produced. Also, possible interaction between ferritin and *P. furiosus* DNA has not yet been explored.

Structural aspects

EPR spectroscopy indicates that, when isolated from *E. coli*, the *P. furiosus* ferritin contains ca. 0.5 Fe per subunit as mononuclear high-spin Fe(III) in a single chemical environment. The significance of this observation is not clear, however, the EPR spectrum is remarkably reminiscent to one reported for wild-type *E. coli* bacterioferritin (Cheesman et al. 1993; Le Brun et al. 1993). That signal was assigned to monomeric iron at or near the putative ferroxidase center (Cheesman et al. 1993; Le Brun et al. 1993). Assignment to the ferroxidase center would imply preferential loading of that center by a single iron as opposed to cooperative binding of two irons (resulting in magnetic coupling and the absence of an EPR signal). Note, however, the complication that not two but three Fe sites have recently been identified in what appears to be the ferroxidase center of *E. coli* ferritin (EcFtnA) (Stillman et al. 2001); also three Fe sites have very recently been found in the 12-mer Dps-ferritin of *H. salinarum* (Reindel et al. 2002; Zeth et al. 2004). Based on the similarity of the EPR spectra, the structure of the mononuclear-binding site in *E. coli* bacterioferritin and *P. furiosus* ferritin should be rather similar. The only site that is fully conserved between the two proteins in terms of Fe ligands is what has been labeled 'A site' (ligands: OOON) in the structure of *E. coli* ferritin (Stillman et al. 2001) with ligands (in *P. furiosus* and *E. coli* numbering) Glu-17, Glu-50, His-53, and one water.

The EPR spectrum of crystalline and/or amorphous core structures is a characteristic fingerprint for iron-loaded ferritin proteins. The spectrum has been interpreted as reflecting superparamagnetism from nano-sized (anti-)ferromagnetic domains above the blocking temperature (Boas et al. 1971; Cheesman et al. 1992; Deighton et al. 1991; Voskoboynik 1997; Wajnberg et al. 2001; Weir et al. 1985). The details of the superparamagnetism will depend on the detailed composition of the nano structures, which in its turn depend on multiple factors, e.g., the extent of iron (and/or other metal ion) loading and the percentage of coincorporated phosphate (and/or other oxoanion). Indeed, a variety of spectral shapes and positions has been observed (Boas et al. 1971; Cheesman et al. 1992; Deighton et al. 1991; Voskoboynik 1997; Wajnberg et al. 2001; Weir et al. 1985); however, the combination of an unusually broad EPR spectrum, extending over a field range of ca. 1 T, with a protein that remains perfectly soluble after loading with a large excess of iron under oxidizing conditions is quite unique for ferritins, and also defines the here described *P. furiosus* protein as a family member.

Hyperthermostability

Ferritins in general are relatively resistant to thermal denaturation. The stability of a protein is a multifaceted property, however, the retainment of biological activity is the ultimate criterion for overall stability. The ferritin from *P. furiosus* appears to be the most thermostable ferritin known so far; the recombinant 24-mer as isolated from *E. coli* fully retains its activity for the process from Fe(II) binding to ferrihydrite core formation after several hours of incubation in boiling water. The activity even withstands autoclaving at 120°C for some time. The protein is thus potentially an interesting model system for studies on the structural basis of hyperthermostability. From a different perspective, the stability of *P. furiosus* ferritin may well have additional value in biotechnology, where a recent surge in activities is seen in the exploration of (thus far mesophilic) ferritin proteins for the construction of nano-sized structures for biocatalytical (Ueno et al. 2004; Zhang et al. 2000), environmental cleaning (Hosein et al. 2004) or nanotechnological (Sleytr et al. 1999; Zhang et al. 2002) purposes.

Acknowledgements We are grateful to prof. Simon de Vries for helpful discussion. We thank prof. Ana Maria Varela Coelho from the ITQB (Oeiras, Portugal) for providing mass spectrometry data. Anton Korteweg from Wageningen University (The Netherlands) is acknowledged for help with differential scanning calorimetry. This research has been financially supported by the Council for Chemical Sciences of the Netherlands Organization for Scientific Research (CW-NWO) under project number 700.51.301.

References

Adams MWW, Jenney FE Jr, Clay MD, Johnson MK (2002) Superoxide reductase: fact or fiction? J Biol Inorg Chem 7:647–652

Almiron M, Link AJ, Furlong D, Kolter R (1992) A novel DNA-binding protein with regulatory and protective roles in starved *Escherichia coli*. Genes Dev 6:2646–2654

Altschul SF, Madden TL, Schaffer AA, Zhang J, Zhang Z, Miller W, Lipman DJ (1997) Gapped BLAST and PSI-BLAST: a new generation of protein database search programs. Nucleic Acids Res 25:3389–3402

Andrews SC, Smith JM, Hawkins C, Williams JM, Harrison PM, Guest JR (1993) Overproduction, purification and characterization of the bacterioferritin of *Escherichia coli* and a C-terminally extended variant. Eur J Biochem 213:329–338

Arendsen AF, Veenhuizen PT, Hagen WR (1995) Redox properties of the sulfhydrogenase from *Pyrococcus furiosus*. FEBS Lett 368:117–121

Baaghil S, Lewin A, Moore GR, Le Brun NE (2003) Core formation in *Escherichia coli* bacterioferritin requires a functional ferroxidase center. Biochemistry 42:14047–14056

Bauminger ER, Harrison PM, Hechel D, Nowik I, Treffry A (1991) Mossbauer spectroscopic investigation of structure-function relations in ferritins. Biochim Biophys Acta 1118:48–58

Boas JF, Troup GJ (1971) Electron spin resonance and Mossbauer effect studies of ferritin. Biochim Biophys Acta 229:68–74

Bonomi F, Kurtz DM, Cui X (1996) Ferroxidase activity of recombinant *Desulfovibrio vulgaris* rubrerythrin. J Biol Inorg Chem 1:67–72

Boyer RF, McCleary CJ (1987) Superoxide ion as a primary reductant in ascorbate-mediated ferritin iron release. Free Radic Biol Med 3:389–395

Carrondo MA (2003) Ferritins, iron uptake and storage from the bacterioferritin viewpoint. EMBO J 22:1959–1968

Cheesman MR, Kadir FH, Al-Basseet J, Al-Massad F, Farrar J, Greenwood C, Thomson AJ, Moore GR (1992) Epr and magnetic circular dichroism spectroscopic characterization of bacterioferritin from *Pseudomonas aeruginosa* and *Azotobacter vinelandii*. Biochem J 286:361–367

Cheesman MR, Le Brun NE, Kadir FH, Thomson AJ, Moore GR, Andrews SC, Guest JR, Harrison PM, Smith JM, Yewdall SJ (1993) Haem and non-haem iron sites in *Escherichia coli* bacterioferritin: spectroscopic and model building studies. Biochem J 292:47–56

Combet C, Blanchet C, Geourjon C, Deleage G (2000) NPS@: network protein sequence analysis. Trends Biochem Sci 25:147–150

Crichton RR (2001) Inorganic biochemistry of iron metabolism: from molecular mechanisms to clinical consequences, 2nd edn. Wiley, Chichester

Dawson MC, Elliott DC, Elliott WH, Jones KM (1986) Data for biochemical research, 3rd edn. Clarendon Press, Oxford

Deighton N, Abu-Raqabah A, Rowland IJ, Symons MCR, Peters TJ, Ward RJ (1991) Electron paramagnetic resonance studies of a range of ferritins and haemosiderins. J Chem Soc Faraday Trans 87:3193–3197

Fiala G, Stetter KO (1986) *Pyrococcus furiosus* sp. nov. represents a novel genus of marine heterotrophic archaebacteria growing optimally at 100°C. Arch Microbiol 145:56–61

Frolow F, Kalb AJ, Yariv J (1994) Structure of a unique twofold symmetric haem-binding site. Nat Struct Biol 1:453–460

Hagedoorn PL, Freije JR, Hagen WR (1999) *Pyrococcus furiosus* glyceraldehyde 3-phosphate oxidoreductase has comparable W(6+/5+) and W(5+/4+) reduction potentials and unusual [4Fe-4S] EPR properties. FEBS Lett 462:66–70

Hagen WR (1992) EPR spectroscopy of iron-sulfur proteins. Adv Inorg Chem 38:165–222

Hempstead PD, Yewdall SJ, Fernie AR, Lawson DM, Artymiuk PJ, Rice DW, Ford GC, Harrison PM (1997) Comparison of the three-dimensional structures of recombinant human H and horse L ferritins at high resolution. J Mol Biol 268:424–448

Hennessy DJ, Reid GR, Smith FE, Thompson SL (1984) Ferene—a new spectrophotometric reagent for iron. Can J Chem 62:721–724

Hosein HA, Strongin DR, Allen M, Douglas T (2004) Iron and cobalt oxide and metallic nanoparticles prepared from ferritin. Langmuir 20:10283–10287

Hudson AJ, Andrews SC, Hawkins C, Williams JM, Izuhara M, Meldrum FC, Mann S, Harrison PM, Guest JR (1993) Overproduction, purification and characterization of the *Escherichia coli* ferritin. Eur J Biochem 218:985–995

Jenney FE Jr, Verhagen MFJM, Cui X, Adams MWW (1999) Anaerobic microbes: oxygen detoxification without superoxide dismutase. Science 286:306–309

Johnson E, Cascio D, Sawaya MR, Gingery M, Schröder I (2005) Crystal structures of a novel tetrahedral open pore ferritin from the hyperthemophilic archaeon *Archaeoglobus fulgidus*. Structure 13:637–648

Le Brun NE, Cheesman MR, Thomson AJ, Moore GR, Andrews SC, Guest JR, Harrison PM (1993) An EPR investigation of non-haem iron sites in *Escherichia coli* bacterioferritin and their interaction with phosphate. A study using nitric oxide as a spin probe. FEBS Lett 323:261–266

Levi S, Cesareni G, Arosio P, Lorenzetti R, Soria M, Sollazzo M, Albertini A, Cortese R (1987) Characterization of human ferritin H chain synthetized in *Escherichia coli*. Gene 51:269–274

Ma K, Adams MWW (1999) A hyperactive NAD(P)H:rubredoxin oxidoreductase from the hyperthermophilic archaeon *Pyrococcus furiosus*. J Bacteriol 181:5530–5533

Matias PM, Tatur J, Carrondo MA, Hagen WR (2005) Crystallization and preliminary X-ray characterization of a ferritin from the hyperthermophilic archaeon and anaerobe *Pyrococcus furiosus*. Acta Cryst F 61:503–506

Pierik AJ, Hagen WR (1991) S = 9/2 EPR signals are evidence against coupling between the siroheme and the Fe/S cluster prosthetic groups in *Desulfovibrio vulgaris* (Hildenborough) dissimilatory sulfite reductase. Eur J Biochem 195:505–516

Pierik AJ, Wolbert RB, Mutsaers PH, Hagen WR, Veeger C (1992) Purification and biochemical characterization of a putative [6Fe-6S] prismane-cluster-containing protein from *Desulfovibrio vulgaris* (Hildenborough). Eur J Biochem 206:697–704

Reindel S, Anemüller S, Sawaryn A, Matzanke BF (2002) The DpsA-homologue of the archaeon *Halobacterium salinarum* is a ferritin. Biochim Biophys Acta 1598:140–146

Rocha ER, Andrews SC, Keen JN, Brock JH (1992) Isolation of a ferritin from *Bacteroides fragilis*. FEMS Microbiol Lett 74:207–212

Romão CV (2003) Iron metabolism in sulfate reducing bacteria. The hemoferritin from *Desulfovibrio desulfuricans* ATCC 27774. PhD Thesis, Universidade Nova de Lisboa

Romão CV, Regalla M, Xavier AV, Teixeira M, Liu MY, Le Gall J (2000) A bacterioferritin from the strict anaerobe *Desulfovibrio desulfuricans* ATCC 27774. Biochemistry 39:6841–6849

Sleytr UB, Messner P, Pum D, Sára M (1999) Crystalline bacterial cell surface layers (S layers): from supramolecular cell structure to biomimetics and nanotechnology. Angew Chem Int Ed 38:1034–1054

Smith JL (2004) The physiological role of ferritin-like compounds in bacteria. Crit Rev Microbiol 30:173–185

Stillman TJ, Hempstead PD, Artymiuk PJ, Andrews SC, Hudson AJ, Treffry A, Guest JR, Harrison PM (2001) The high-resolution X-ray crystallographic structure of the ferritin (EcFtnA) of *Escherichia coli*; comparison with human H ferritin (HuHF) and the structures of the Fe(3+) and Zn(2+) derivatives. J Mol Biol 307:587–603

Tempel W, Liu ZJ, Schubot FD, Shah A, Weinberg MV, Jenney FE Jr, Arendall WB III, Adams MWW, Richardson JS, Richardson DC, Rose JP, Wang BC (2004) Structural genomics of *Pyrococcus furiosus*: X-ray crystallography reveals 3D domain swapping in rubrerythrin. Proteins 57:878–882

Thompson JD, Higgins DG, Gibson TJ (1994) CLUSTAL W: improving the sensitivity of progressive multiple sequence alignment through sequence weighting, position-specific gap penalties and weight matrix choice. Nucleic Acids Res 22:4673–4680

Treffry A, Harrison PM (1978) Incorporation and release of inorganic phosphate in horse spleen ferritin. Biochem J 171:313–320

Ueno T, Suzuki M, Goto T, Matsumoto T, Nagayama K, Watanabe Y (2004) Size-selective olefin hydrogenation by a Pd nanocluster provided in an apo-ferritin cage. Angew Chem Int Ed 43:2527–2530

Voskoboynik U (1997) Anomalous field dependence of blocking temperature of natural horse-spleen ferritin. Acta Phys Pol A 92

Wajnberg E, El-Jaick LJ, Linhares MP, Esquivel DM (2001) Ferromagnetic resonance of horse spleen ferritin: core blocking and surface ordering temperatures. J Magn Reson 153:69–74

Weir MP, Peters TJ, Gibson JF (1985) Electron spin resonance studies of splenic ferritin and haemosiderin. Biochim Biophys Acta 828:298–305

Zeth K, Offermann S, Essen LO, Oesterhelt D (2004) Iron-oxo clusters biomineralizing on protein surfaces: structural analysis of *Halobacterium salinarum* DpsA in its low- and high-iron states. Proc Natl Acad Sci USA 101:13780–13785

Zhang N, Fengyi L, Fu QJ, Tsang SC (2000) Naturally occurring ferritin as a novel catalyst for selective hydroxylation of phenol. React Kinet Catal Lett 71:393–404

Zhang Y, Li Y, Wang D, Dai H (2002) Imaging as-grown single-walled carbon nanotubes originated from isolated catalytic nanoparticles. Appl Phys A 74:325–328

Zhao G, Ceci P, Ilari A, Giangiacomo L, Laue TM, Chiancone E, Chasteen ND (2002) Iron and hydrogen peroxide detoxification properties of DNA-binding protein from starved cells A ferritin-like DNA-binding protein of *Escherichia coli*. J Biol Chem 277:27689–27696